CIELAB – Spectral image MATCHING: An app for merging colorimetric and spectral images for grapes and derivatives

Rodríguez-Pulido, Francisco J.; rpulido@us.es
https://orcid.org/0000-0002-8230-2015;
Gordillo, Belén; bgordillo@us.es
https://orcid.org/0000-0003-2986-7911;
González-Miret, M. Lourdes*; miret@us.es
https://orcid.org/0000-0003-0572-051X;
Heredia, Francisco J.; heredia@us.es
https://orcid.org/0000-0002-3849-8284;

Food Colour and Quality Lab., Área de Nutrición y Bromatología, Facultad de Farmacia, Universidad de Sevilla, 41012 Sevilla, Spain.

*Corresponding author:
González-Miret, M. Lourdes
Food Colour & Quality Laboratory, Dept. Nutrition & Food Science. Facultad de Farmacia. Universidad de Sevilla. 41012-Sevilla, Spain
Tel.: +34 955420938
e-mail: miret@us.es

ABSTRACT

Imaging techniques have revolutionised the way quality is assessed in food products. Using cameras, it is possible to estimate not only the chemical composition of a product but also its geometric distribution. However, the limited range of detectors implies the use of different measuring equipment. The presence of small and discrete samples or very heterogeneous samples makes joining both sets of data a complicated task. This work arises from the need to merge images with colour information and NIR spectral information on grape samples and derivatives. An application has been created under MATLAB to join this type of images so that it is possible to simultaneously extract the colour and/or spectral information of each pixel or object present in the image. Although the software can be used in a wide range of applications, it has been successfully applied to grape and grape seed samples. In red grape bunches, it was possible to evaluate individually grapes and notice differences due to changes in visible and infrared regions at the same time. In the case of white grape seeds, it was proved that merged images were better to discriminate between varieties than the single CIELAB or spectral images.

KEYWORDS

CIELAB; NIR; Spectral Imaging; Image Matching; MATLAB.

1. INTRODUCTION

Colour and appearance, as the first attributes that consumers perceive, have been the features most characterized in food products (Fernández-Vázquez et al., 2011). Historically, these analyses have been done through sensory analysis, which over the years has been replaced by instrumental measurements, mainly due to the need to automate inspection processes in the food industry. Advances in technology have led to the emergence of devices capable of analysing in real-time and transmitting the results online for rapid decision making. So much so that, the use of Precision Agriculture is the only viable way to manage the needs of such an overpopulated world (Singh and Singh, 2020).

Of all the devices available for rapid analysis in agriculture, those based on Computer Vision are worth mentioning (Ma et al., 2016). There is an *ad hoc* application for the evaluation of any type of product. Mangoes (Wendel et al., 2018), grapes (Nogales-Bueno et al., 2015b), asparagus (Donis-González and Guyer, 2016), coffee beans (de Oliveira et al., 2016), or figs (Benalia et al., 2016) are good examples of products whose agrological and physicochemical characteristics are quite different and which already have a solution of imaging techniques to be evaluated.

1.1. Imaging Techniques

Since the creation of the first computer, human beings have dreamed of creating machines capable of relating to their environment in the same way their senses do. Making a machine capable of seeing has been one of the great challenges of electronics. Simply creating cameras was not enough. We needed machines that could understand what they were seeing. All the advances in optical systems have made Computer Vision one of the techniques with the greatest field of application in the food industry. Depending on the measurement geometry and the type of information obtained we will differentiate between conventional RGB images and spectral images.

1.1.1. *RGB imaging*

Conventional RGB cameras are usually built with silicon-based detectors with filters so that each point only receives information from one of the three primary colours. The big problem with these cameras is that RGB or HSI colour spaces are device-dependent, so in principle, they cannot be used for absolute colour measurements (Yam and Papadakis, 2004). Despite these limitations, many authors still use these colour spaces. By controlling all environmental factors and through chemometrics tools it is possible to predict physicochemical characteristics in food products from these colour data. Other authors use the CIELAB transformation that graphic editing programs offer. This transformation only depends on the original values of RGB, thus they always make a systematic error. If the final aim is not the colorimetric measurement but the physicochemical analysis through chemometrics, this error has no further importance. The most orthodox method is to follow the recommendations of CIE and use not device-dependent colour spaces (CIE, 2004). The most used colour space in food products analysis is CIE 1976 (L*a*b*) or simply: CIELAB. However, conversion between RGB and CIELAB requires long calibration processes utilizing standard illumination and reference materials (León et al., 2006). This is the only method when the goal is to get absolute colorimetric measurements by means of RGB cameras.

1.1.2. *Spectral imaging*

Spectral imaging technology appeared in the mid-1980s. This revolution, that began with airborne images and which could be applied to several fields, was appointed as “hyperspectral imaging”. Almost forty years later, this technology cannot be longer mentioned as groundbreaking, but its applications continue growing nowadays. Now that the technique is well implemented, experts recommend the use of more appropriated terms such as “imaging spectroscopy” or “spectral imaging” (Polder and Gowen, 2020). Spectral images are three-dimensional data matrix where the first two axes (x and y) of the matrix represent the spatial coordinates, while the third (λ) axis depicts the spectral dimension. They can be visualised as hundreds of single grayscale images of the same scene, where each image represents a single band that may be as narrow as the equipment allows.

1.2. Image Analysis and Viticulture

The wine industry has relevant importance within food science. To obtain quality wines it is necessary to control the cultivation at all levels. For this reason, there are methods for evaluating vines, soil, foliage, and fruit, among others. Even within the fruit of the vine, it is necessary to control different parts such as seed, pulp, and skin. Imaging techniques have been successfully applied to these parts over the last ten years. Detection of flowering (Palacios et al., 2020), determination of soil quality (Retzlaff et al., 2015), leaf characterization (Diago et al., 2013), grape marc composition (Jara-Palacios et al., 2016), ripeness of berries and seeds (Rodríguez-Pulido et al., 2012), or grape composition (Nogales-Bueno et al., 2015a) are some examples of these applications.

1.3. Complementarity of techniques and objective of the work

There is not a universal optical sensor capable of recording information from many regions of the electromagnetic spectrum at the same time. Therefore, depending on the characteristics to be measured on the samples, the type of sensor must be chosen correctly. The most common detectors are CCD, whose spectral range depends on whether it is cooled or not, CMOS or InGaAs. Silicon-based detectors such as CCD and CMOS have sensitivities up to 1000 nm. Those based on InGaAs have no sensitivity in the visible but reach wavelengths of 1700 nm (Huang et al., 2017). Besides, detectors can be matrix or linear, the latter needing a brooming system to acquire a complete image.

In many studies, it is common to simultaneously determine characteristics by different optical techniques. When using point spectroscopy this task is as simple as measuring the same sample by different techniques and then joining the information obtained. This task is more challenging when it refers to imaging techniques. Imaging techniques are preferably used when the optical characteristics of the image vary according to the area of the sample being measured. In this case, it is difficult to join the information from different techniques, since the optical characteristics vary drastically, and it is not possible to simply superimpose the matrices that comprise each type of image. Furthermore, this task would be limited for reasons as simple as differences in resolution and framing.

When using RGB images, the task of joining images with common elements is completely solved. The process by which two images with common elements are merged is called "image matching" or "image stitching". There are numerous computer programs capable of performing this process quickly and reliably. In fact, research is still underway to improve the algorithms, which are increasingly robust to changes in light and perspective, and to improve the resulting images (Laraqui et al., 2015; Wang and Yang, 2020). All systems of airborne or satellite spectral images include their own stitching procedure to merge their captures for obtaining a whole complete image of the scanned region. The problem arises when it is necessary to merge data obtained from very different imaging techniques.

This work stems from the need for evaluating jointly NIR spectral images and images obtained from a conventional imaging system. To our knowledge, there is not an available application to make this task. Therefore, this work has aimed to develop a simple application that allows researchers to get in a single spectral image both colorimetric and NIR data.

2. MATERIALS AND METHODS

2.1. Programming language

The App Designer tool included in MATLAB R2020a has been used for this work (The Mathworks, 2020). MATLAB (short for Matrix Laboratory) is a mathematical software tool widely used in the scientific field and is characterised by its use of a friendly language for those researchers without extensive programming experience. Its main feature is the ease with which the program manipulates matrices. This is very useful in image analysis since both digital images and spectral images can be considered three-dimensional matrices.

2.2. Starting images

2.2.1. *CIELAB images*

These images were acquired with the DigiEye® imaging System (Verivide, UK) (Luo et al., 2001). This equipment is specially designed for colour measurement according to CIE guidelines and the evaluation of appearance. The equipment consists of a dome lighting booth with two D65 standard illuminant emulators lamps, a Nikon® D80 reflex camera and a computer that controls the equipment. The output images are stored in TIF files (57.4 MB) that have a resolution of 3872×2592 pixels which each contains *L*a*b** colour coordinates stored in 16-bit data per channel.

2.2.2. *Spectral Images*

The system comprised a Xenics® XEVA-USB InGaAs camera (320×256 pixels; Xenics Infrared Solutions, Inc., Leuven, Belgium), a spectrograph (Specim ImSpector N17E Enhanced; Spectral Imaging Ltd., Oulu, Finland) covering the spectral range between 884 and 1717 nm (spectral resolution of 3.25 nm), two 70 W tungsten iodine halogen lamps (Prilux®, Barcelona, Spain) used as light source, a mirror scanner (Spectral Imaging Ltd., Oulu, Finland), and a computer system. Images were recorded using a 50 Hz frame rate and an exposure time of 9 ms using the instrument acquisition software SpectralDAQ 3.62 (Spectral Imaging Ltd., Oulu, Finland). Once the images are acquired, ‘white reference’ and ‘dark reference’ images were also recorded to calibrate the signal according to the equation $R=(R_0–D)/(W–D)$, being D the dark signal, W the white reference signal and R_0 the RAW data. In this work, the relative reflectance spectrum obtained after calibration was used for the calibration processes. No spectroscopic transformation treatments or other spectral pre-treatments were performed. Each calibrated spectral image is composed of two files. First one is a DAT file (75 MB) that contains the binary data of the cube. For its reading, a header HDR file (3 KB) is also needed. This header has the metadata associated with the binary file. The content is variable, but it usually has the size, data type, and the wavelength that belongs to each band.

3. RESULTS AND DISCUSSION

3.1. Design of Graphical User Interface

Figure 1 shows a layout of the Graphical User Interface (GUI). Its design consists of a single screen that contains all the controls for its functioning and can be divided into the following parts. At the top, there are two areas in parallel for displaying CIELAB and spectral images. Between them, there are the buttons and controls to prepare the images before matching. In the middle, there is a panel with the “match” button and the options to export the resulting image. Below this section, there are the steps that indicate the status of the process and alerts about the possible troubles found in it. And finally, at the bottom, there are the log of the program and the buttons to reset and exit.

3.2. Functioning

3.2.1. *Loading a pair of images*

The ‘load’ button opens a pop-up dialogue box for opening the CIELAB image. It automatically reads the spectral image if it has the same name. In the case it has not, a new dialogue box will request the location of the spectral file. This spectral file must have the corresponding header to be opened. The two parallel windows show a preview of both images. For CIELAB image, it can be visualized as a regular RGB image or with any of the five colorimetric coordinates in greyscale: L^* (lightness), a^*, b^*, C^*_{ab} (chroma) or h_{ab} (hue). In the case of the spectral image, a slider allows browsing along the range of wavelengths available. A specific band can be also fixed in an edit field.

3.2.2. *Cropping and Segmentation*

Some images may contain big background areas or non-desirable elements. This only will increase the computing workload. Therefore, ‘Crop image’ button will allow us to cut them by clicking and dragging a selection box around the regions of interest. The goal of this task is to reduce the information to the sample with the minimum of surrounding background.

The ‘Segmentation’ button will identify the sample in both images and display the segmentation mask for each one. The segmentation process is based on a k-means algorithm that collects all the pixels from the two images and categorises them into two groups. For the CIELAB image it uses as input the L*a*b* data and for the spectral image it samples one every ten spectral bands. In this last case, the algorithm calculates previously the first derivative of the signal. This enhances the results when there are parts of the background surface inconsistently illuminated. To find out which category belongs to which group, the programmed algorithm inspects the pixels at the cropped image boundaries, regions that will always belong to the background.

3.2.3. *Straightening*

Both images, CIELAB and spectral, may have very different resolutions and sizes. Also, the frame of the captures may not have had the same angle. For these reasons, at this point in the process, it must be decided whether it is the CIELAB image that will be modified to adapt in resolution and straightening to the spectral image, or vice versa. The image to straighten will be selected by switching between two radio buttons. Then, ‘Adjust angle’ will straighten the alignment of the sample before matching. If the image is completely rotated to each other, a check box will amend this point. Otherwise, if there is no angle to correct, the user only must select the image to adapt and click on 'Skip adjust'. In any case, both windows will show previsualization of the steps before matching.

3.2.4. *Match and export*

In this point of the process, both images are ready to be matched. Based on the segmentation masks created previously, the algorithm resizes and re-crops the image to adapt it to the other. To adjust the new resolution, every output pixel value in resizing is a weighted average of pixels in the nearest 2-by-2 neighbourhood. The merged image will be saved as a new spectral image. There are some checkboxes to select the desired information to export. The segmentation mask, RGB, CIELAB in different formats and the whole or a specific range of the spectrum can be stored in an image that will be saved with the original name with the suffix '_matched'. This name can be also modified in an edit field.

The software developed can be used in a wide range of fields. Notwithstanding, we have successfully applied it in our research in viticulture.

3.3. Examples of application

3.3.1. *Application to white grape seeds*

In this essay, we used samples of grape seeds (*Vitis vinifera* L.) of two white varieties (cv. Moscatel and cv. Pedro Ximénez). There is an heterogeneity that occurs naturally along the whole maturation process (Quijada-Morín et al., 2016). For this reason, it is not easy to discriminate between varieties when only seeds are measured. Separately, colorimetric and spectral datasets have already been successfully applied to perform this task (Rodríguez-Pulido et al., 2012, 2013). Anyway, if colour and NIR spectrum want to be simultaneously measured in each seed we must consider each one as a sample unit. Due to the small size and the chaotic distribution of seeds on a sample tray, it would be very difficult to pair both datasets; nevertheless, this was easily performed with the application developed. Figure 2 shows four samples of groups of seeds (419 single seeds). Those at the top belong to Moscatel (MO) and those at the bottom to Pedro Ximénez (PX). This is the representation of the image acquired with DigiEye. The spectral image of each sample was also acquired and then, they were matched with the application. Employing an algorithm made with MATLAB, the information of each seed was extracted, which contained both colorimetric and NIR spectral data. Considering the variety as a categorical variable, we applied three Linear Discriminant Analyses (LDA), depending on the matrix used as independent variables. The first one used only CIELAB coordinates, the second used only NIR spectral values and the last one used the blend of these two. Table 1 shows the classification matrix of each LDA. If we consider each of the grape varieties, MO variety is better classified than the PX when the colorimetric data is used. When using only NIR, PX seeds are more accurately classified than MO seeds. The linkage of spectral data to the colour data has hardly any increase in accuracy compared to the use of colour data for the MO variety. On the contrary, for the PX variety, the increase in accuracy is up to six per cent higher compared to using colour data alone.

3.3.2. *Application to red grape bunches*

In this second essay, we acquired images of grape (*Vitis vinifera* L.) bunches of two red varieties (27 of cv. Syrah and 22 of cv. Tempranillo). Sampling was carried out from the start of veraison until one week after harvesting. In this case, we show a pair of images representing the beginning and the end of sampling. CIELAB and spectral images were successfully matched with the software created. According to the selected options, the new cube of data contained the segmentation mask, RGB values, CIELAB and spectral information. Then, a Principal Component Analysis (PCA) was applied to the layers belonging to CIELAB and spectral data separately. In order to see the whole information at a glance, this was represented as an image that contained the main Principal Components in each RGB channel. Thus, differences in the pseudo-colour image showed differences in the input database used in the PCA model (Figure 3). At the top, there is a common RGB image to see the actual appearance of both bunches. In the middle, PCA results of the CIELAB data are shown. As it was expected, there is a high correlation between top and middle images. In this analysis, h_{ab} was the colorimetric coordinate with the most influence in PC1 (red channel), b* and C_{ab}* had almost the same influence in PC2 and, eventually, L* was the coordinate with the highest loading in PC3. Yellowish areas in the middle image in Figure 3 implies high scores in PC1 and PC2. At the bottom, there are the PCA results when only the NIR spectrum is considered. It is possible to notice differences in grapes, but it is not so conditioned by the appearance of them. In this new image, wavelengths between 1100-1200 nm and around 1400 nm had the most influence in PC1, PC2, and PC3, represented by RGB, respectively. These regions are in agreement with Hernández-Hierro et al. (2013). According to literature, colour changes during the veraison are due to the loss of chlorophylls and the biosynthesis of anthocyanins in the skins. Once the veraison is complete, the chemical composition of grapes continues towards the increase of sugars in the pulp as well as the evolution of phenolic compounds. These last changes have not to impact in the appearance (Ristic and Iland, 2005; Rolle et al., 2009; Zsófi et al., 2014). Nogales-Bueno et al. (2015c) proved that the union of colorimetric and spectral data improve the goodness of fit in quantitative analyses. With these new spectral cubes, which have all data available at each pixel, chemometric models can give more weight to those variables that are most useful in prediction models, especially when stepwise regression models are used.

This tool was also used for detecting fully ripe grapes. From each image of bunches belonging to Tempranillo and Syrah varieties along the maturation, the sugar concentration in must was measured in five grapes randomly picked in each sample with a portable refractometer at 20 ºC. Colorimetric and NIR images were acquired in the same session. For building models and after merging the images, data from points were collected from each grape using a 21-pixel grid. In turn, these points were labelled regarding this ripeness (Figure 4). In total, there were collected 1827 pixels from 87 fully ripe grapes and 3328 pixels from 158 underripe grapes. As in the case of seeds, three Linear Discriminant Analyses (LDA) were performed, depending on the matrix used as independent variables: CIELAB, NIR, and the blend of these two by using the software developed. Moreover, since it was a huge amount of data, samples were split into calibration (75%) and prediction (25%) sets. Table 2 shows the classification matrix of each LDA for the prediction set. Colorimetric data had a high potential for predicting underripe grapes. This happened because veraison is a phenomenon that occurs much before the technological maturity in grapes. All green grapes are consequentially underripe. Conversely, once the colour has changed, it is not possible to assess whether the grape has reached the desired level of sugars. This is the reason why only 48.3 % of fully ripe grapes are correctly classified. If we consider NIR data, where colour has no influence, the classification is correct for 80% of the samples, approximately. Moreover, this percentage is almost the same for the two classes. In the last case, where both kinds of data were simultaneously considered, the percentage of correct classification reached 93.6%. The classification was better for both underripe and fully ripe grapes when comparing with previous LDA results. It is worth mentioning that the synergy demonstrated between the two techniques has been made possible by the point-to-point comparison within the images, which would be very difficult to obtain with conventional spectroscopic techniques or with the separate imaging techniques.

4. CONCLUSIONS

The software developed in this study solves an analytical problem when wanting to combine colorimetric and spectral data using imaging techniques. Although the synergy between optical techniques was already demonstrated, this new tool allows the evaluation of discrete samples and those in which there is a certain optical heterogeneity. The simultaneous availability of data allows chemometric techniques to discern in each case the weight of the variables in the prediction models. This application has proved useful whenever images obtained in the laboratory are considered, under controlled environmental conditions and always using smooth and homogeneous surfaces as a sample background. Although these conditions can be easily reproduced in industrial food control processes, the future of the application should focus on the possibility of processing images acquired in more complex environments.

ACKNOWLEDGMENTS

We are indebted to Programa Operativo FEDER Andalucía 2014-2020 [Ref: US-1261752] and Ministerio de Economía y Competitividad, Spain [Project

AGL2017-84793-C2] for financial support. Also, authors are grateful to Consejo Regulador Condado de Huelva (Bollullos Par del Condado, Huelva, Spain) for the supply of samples, and technical staff of Biology Service (SGI, Universidad de Sevilla) for technical assistance. Francisco J. Rodríguez-Pulido also wants to thank to the UX designer, Christian Cabrera, for the advising during the design of the Graphical User Interface.

REFERENCES

Benalia, S., Cubero, S., Prats-Montalbán, J.M., Bernardi, B., Zimbalatti, G., Blasco, J., 2016. Computer vision for automatic quality inspection of dried figs (Ficus carica L.) in real-time. Comput. Electron. Agric. 120, 17–25. https://doi.org/10.1016/j.compag.2015.11.002

CIE (Ed.), 2004. Colorimetry, 3. ed. ed, Technical report / CIE. CIE, Central Bureau, Vienna.

de Oliveira, E.M., Leme, D.S., Barbosa, B.H.G., Rodarte, M.P., Pereira, R.G.F.A., 2016. A computer vision system for coffee beans classification based on computational intelligence techniques. J. Food Eng. 171, 22–27. https://doi.org/10.1016/j.jfoodeng.2015.10.009

Diago, M.P., Fernandes, A.M., Millan, B., Tardaguila, J., Melo-Pinto, P., 2013. Identification of grapevine varieties using leaf spectroscopy and partial least squares. Comput. Electron. Agric. 99, 7–13. https://doi.org/10.1016/j.compag.2013.08.021

Donis-González, I.R., Guyer, D.E., 2016. Classification of processing asparagus sections using color images. Comput. Electron. Agric. 127, 236–241. https://doi.org/10.1016/j.compag.2016.06.018

Fernández-Vázquez, R., Stinco, C.M., Meléndez-Martínez, A.J., Heredia, F.J., Vicario, I.M., 2011. Visual and Instrumental Evaluation of Orange Juice Color: A Consumers' Preference Study. J. Sens. Stud. 26, 436–444. https://doi.org/10.1111/j.1745-459X.2011.00360.x

Hernández-Hierro, J.M., Nogales-Bueno, J., Rodríguez-Pulido, F.J., Heredia, F.J., 2013. Feasibility Study on the Use of Near-Infrared Hyperspectral Imaging for the Screening of Anthocyanins in Intact Grapes during Ripening. J. Agric. Food Chem. 61, 9804–9809. https://doi.org/10.1021/jf4021637

Huang, L., Zhou, Y., Meng, L., Wu, D., He, Y., 2017. Comparison of different CCD detectors and chemometrics for predicting total anthocyanin content and antioxidant activity of mulberry fruit using visible and near infrared hyperspectral imaging technique. Food Chem. 224, 1–10. https://doi.org/10.1016/j.foodchem.2016.12.037

Jara-Palacios, M.J., Rodríguez-Pulido, F.J., Hernanz, D., Escudero-Gilete, M.L., Heredia, F.J., 2016. Determination of phenolic substances of seeds, skins and stems from white grape marc by near-infrared hyperspectral imaging: Hyperspectral marc analysis. Aust. J. Grape Wine Res. 22, 11–15. https://doi.org/10.1111/ajgw.12165

Laraqui, M., Saaidi, A., Mouhib, A., Abarkan, M., 2015. Images Matching Using Voronoï Regions Propagation. 3D Res. 6, 27. https://doi.org/10.1007/s13319-015-0056-5

León, K., Mery, D., Pedreschi, F., León, J., 2006. Color measurement in L*a*b* units from RGB digital images. Food Res. Int., Physical Properties VI 39, 1084–1091. https://doi.org/10.1016/j.foodres.2006.03.006

Luo, M.R., Cui, G.H., Li.C;, 2001. British Patent entitled Apparatus and method for measuring colour (DigiEye System), Derby University Enterprises Limited.

Ma, J., Sun, D.-W., Qu, J.-H., Liu, D., Pu, H., Gao, W.-H., Zeng, X.-A., 2016. Applications of Computer Vision for Assessing Quality of Agri-food Products: A Review of Recent Research Advances. Crit. Rev. Food Sci. Nutr. 56, 113–127. https://doi.org/10.1080/10408398.2013.873885

Nogales-Bueno, J., Ayala, F., Hernández-Hierro, J.M., Rodríguez-Pulido, F.J., Echávarri, J.F., Heredia, F.J., 2015a. Simplified Method for the Screening of Technological Maturity of Red Grape and Total Phenolic Compounds of Red Grape Skin: Application of the Characteristic Vector Method to Near-Infrared Spectra. J. Agric. Food Chem. 63, 4284–4290. https://doi.org/10.1021/jf505870s

Nogales-Bueno, J., Baca-Bocanegra, B., Rodríguez-Pulido, F.J., Heredia, F.J., Hernández-Hierro, J.M., 2015b. Use of near infrared hyperspectral tools for the screening of extractable polyphenols in red grape skins. Food Chem. 172, 559–564. https://doi.org/10.1016/j.foodchem.2014.09.112

Nogales-Bueno, J., Rodríguez-Pulido, F.J., Heredia, F.J., Hernández-Hierro, J.M., 2015c. Comparative study on the use of anthocyanin profile, color image analysis and near-infrared hyperspectral imaging as tools to discriminate between four autochthonous red grape cultivars from La Rioja (Spain). Talanta 131, 412–416. https://doi.org/10.1016/j.talanta.2014.07.086

Palacios, F., Bueno, G., Salido, J., Diago, M.P., Hernández, I., Tardaguila, J., 2020. Automated grapevine flower detection and quantification method based on computer vision and deep learning from on-the-go imaging using a mobile sensing platform under field conditions. Comput. Electron. Agric. 178. https://doi.org/10.1016/j.compag.2020.105796

Polder, G., Gowen, A., 2020. The hype in spectral imaging. J. Spectr. Imaging. https://doi.org/10.1255/jsi.2020.a4

Quijada-Morín, N., García-Estévez, I., Nogales-Bueno, J., Rodríguez-Pulido, F.J., Heredia, F.J., Rivas-Gonzalo, J.C., Escribano-Bailón, M.T., Hernández-Hierro, J.M., 2016. Trying to set up the flavanolic phases during grape seed ripening: A spectral and chemical approach. Talanta 160, 556–561. https://doi.org/10.1016/j.talanta.2016.07.064

Retzlaff, R., Molitor, D., Behr, M., Bossung, C., Rock, G., Hoffmann, L., Evers, D., Udelhoven, T., 2015. UAS-based multi-angular remote sensing of the effects of soil management strategies on grapevine. J. Int. Sci. Vigne Vin 49, 85–102. https://doi.org/10.20870/oeno-one.2015.49.2.91

Ristic, R., Iland, P.G., 2005. Relationships between seed and berry development of Vitis Vinifera L. cv Shiraz: Developmental changes in seed morphology and phenolic composition. Aust. J. Grape Wine Res. 11, 43–58. https://doi.org/10.1111/j.1755-0238.2005.tb00278.x

Rodríguez-Pulido, F.J., Barbin, D.F., Sun, D.-W., Gordillo, B., González-Miret, M.L., Heredia, F.J., 2013. Grape seed characterization by NIR hyperspectral imaging. Postharvest Biol. Technol. 76, 74–82. https://doi.org/10.1016/j.postharvbio.2012.09.007

Rodríguez-Pulido, F.J., Gómez-Robledo, L., Melgosa, M., Gordillo, B., González-Miret, M.L., Heredia, F.J., 2012. Ripeness estimation of grape berries and seeds by image analysis. Comput. Electron. Agric. 82, 128–133. https://doi.org/10.1016/j.compag.2012.01.004

Rolle, L., Torchio, F., Giacosa, S., Gerbi, V., 2009. Modifications of mechanical characteristics and phenolic composition in berry skins and seeds of Mondeuse winegrapes throughout the on-vine drying process. J. Sci. Food Agric. 89, 1973–1980. https://doi.org/10.1002/jsfa.3686

Singh, N., Singh, A.N., 2020. Odysseys of agriculture sensors: Current challenges and forthcoming prospects. Comput. Electron. Agric. 171, 105328. https://doi.org/10.1016/j.compag.2020.105328

The Mathworks, 2020. MATLAB. The Mathworks Inc., Natik, USA.

Wang, Z., Yang, Z., 2020. Review on image-stitching techniques. Multimed. Syst. 26, 413–430. https://doi.org/10.1007/s00530-020-00651-y

Wendel, A., Underwood, J., Walsh, K., 2018. Maturity estimation of mangoes using hyperspectral imaging from a ground based mobile platform. Comput. Electron. Agric. 155, 298–313. https://doi.org/10.1016/j.compag.2018.10.021

Yam, K.L., Papadakis, S.E., 2004. A simple digital imaging method for measuring and analyzing color of food surfaces. J. Food Eng., Applications of computer vision in the food industry 61, 137–142. https://doi.org/10.1016/S0260-8774(03)00195-X

Zsófi, Zs., Villangó, Sz., Pálfi, Z., Tóth, E., Bálo, B., 2014. Texture characteristics of the grape berry skin and seed (Vitis vinifera L. cv. Kékfrankos) under postveraison water deficit. Sci. Hortic. 172, 176–182. https://doi.org/10.1016/j.scienta.2014.04.008

FIGURE CAPTIONS

Figure 1. Layout of the Graphical User Interface (GUI).

Figure 2. RGB images of grape seeds. The two upper ones are Moscatel (MO) and the lower ones are Pedro Ximénez (PX).

Figure 3. Top, the actual appearance of grape bunches; middle, PCA of colorimetric data; and bottom, PCA of NIR spectral data.

Figure 4. Detail of an image of a grape bunch and the 21-pixel grid used to extract both colourimetric and spectral information from the merged images. In green, pixels of unripe grapes and, in red, pixels of overripe grapes.

HIGHLIGHTS

- A new software was developed for merging colorimetric and NIR spectral images.
- New resulting images allow getting the CIELAB information and NIR spectrum from any pixel at the same time.
- This program has been successfully applied to grape bunches and grape seeds images

Figure 1

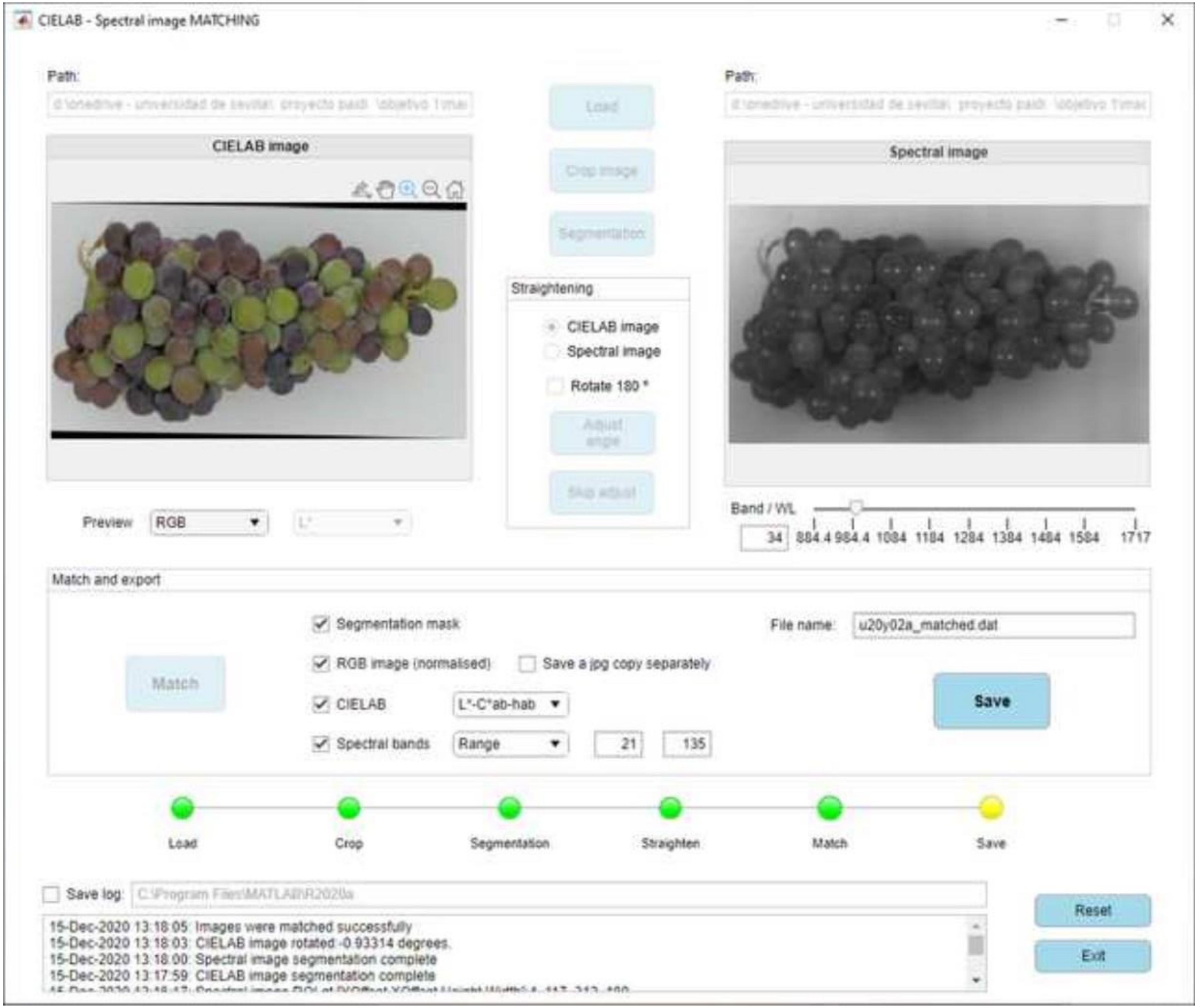
CIELAB - Spectral image MATCHING
Path:
Path:
CIELAB image
Spectral image
Straightening
CIELAB image
Spectral image
Rotate 180 °
Preview
RGB
Band / WL
34
884.4
984.4
1084
1184
1284
1384
1484
1584
1717
Match and export
Segmentation mask
RGB image (normalised)
Save a jpg copy separately
CIELAB
L*-C*ab-hab
Spectral bands
Range
21
135
File name:
u20y02a_matched.dat
Save
Match
Load
Crop
Segmentation
Straighten
Match
Save
Save log
15-Dec-2020 13:18:05 Images were matched successfully
15-Dec-2020 13:18:03 CIELAB image rotated -0.93314 degrees.
15-Dec-2020 13:18:00 Spectral image segmentation complete
15-Dec-2020 13:17:59 CIELAB image segmentation complete
Reset
Exit

Figure 2

Click here to access/download;Figure;FJRP-Image_Matching-Figure2.tif

Figure 3

Click here to access/download;Figure;FJRP-Image_Matching-Figure3.jpg

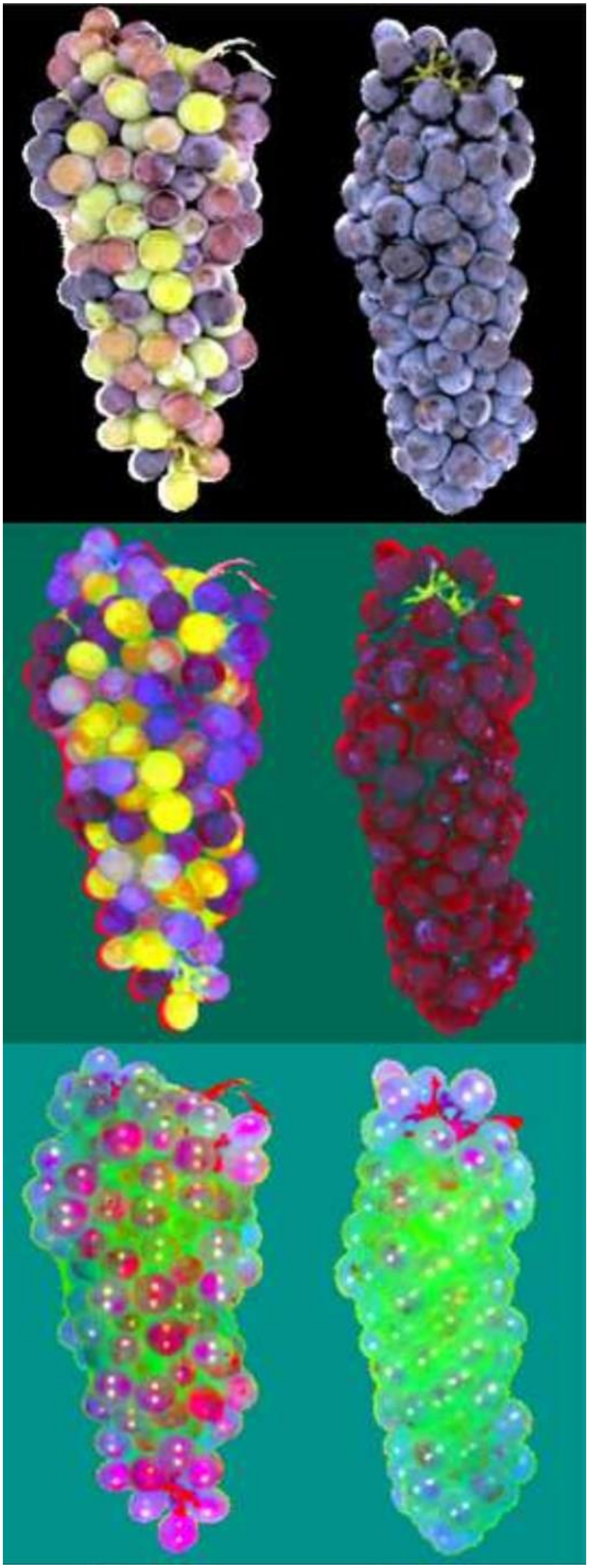

Table 1. Classification matrices after LDA using CIELAB, NIR and CIELAB + NIR as independent variables for predicting the variety of grape seeds.

CIELAB	Percent	*MO*	*PX*
MO	*92.1%*	176	15
PX	*88.6%*	26	202
Total	*90.2%*	202	217

NIR	Percent	*MO*	*PX*
MO	*79.6%*	152	39
PX	*80.7%*	44	184
Total	*80.2%*	196	223

CIELAB + NIR	Percent	*MO*	*PX*
MO	*92.7%*	177	14
PX	*94.3%*	13	215
Total	*93.6%*	190	229

Table 2. Classification matrices after LDA using CIELAB, NIR and CIELAB + NIR as independent variables for predicting the ripeness of grapes.

CIELAB	Percent	*Underripe*	*Fully ripe*
Underripe	*84.3%*	384	72
Fully ripe	*48.3%*	429	401
Total	*73.8%*	813	473

NIR	Percent	*Underripe*	*Fully ripe*
Underripe	*79.6%*	363	93
Fully ripe	*80.7%*	160	670
Total	*80.2%*	523	763

CIELAB + NIR	Percent	*Underripe*	*Fully ripe*
Underripe	*92.7%*	423	33
Fully ripe	*94.3%*	47	783
Total	*93.6%*	470	816

Conflict of Interest and Authorship Conformation Form

Please check the following as appropriate:

- ✓ All authors have participated in (a) conception and design, or analysis and interpretation of the data; (b) drafting the article or revising it critically for important intellectual content; and (c) approval of the final version.

- ✓ This manuscript has not been submitted to, nor is under review at, another journal or other publishing venue.

- ✓ The authors have no affiliation with any organization with a direct or indirect financial interest in the subject matter discussed in the manuscript

- ✓ The following authors have affiliations with organizations with direct or indirect financial interest in the subject matter discussed in the manuscript:

Author's name	Affiliation
Francisco J. Rodríguez-Pulido / Universidad de Sevilla, Spain	
Belén Gordillo / Universidad de Sevilla, Spain	
Francisco J. Heredia / Universidad de Sevilla, Spain	
M. Lourdes González-Miret / Universidad de Sevilla, Spain	

Francisco J. Rodríguez-Pulido: Investigation, Software.

Belén Gordillo: Investigation, Conceptualization.

M. Lourdes González-Miret: Writing - Review & Editing.

Francisco J. Heredia: Conceptualization, Supervision.